

HaLoRA: Hardware-aware Low-Rank Adaptation for Large Language Models Based on Hybrid Compute-in-Memory Architecture

Taiqiang Wu^{1†}, Chenchen Ding^{1†}, Wenyong Zhou^{1†},
Yuxin Cheng¹, Xincheng Feng¹, Shuqi Wang¹, Chufan Shi², Zhengwu Liu^{1*}, and Ngai Wong^{1*}

¹*The University of Hong Kong* ²*Tsinghua University*

takiwu@connect.hku.hk, nwong@eee.hku.hk

Abstract—Low-rank adaptation (LoRA) is a predominant parameter-efficient finetuning method to adapt large language models (LLMs) for downstream tasks. In this paper, we first propose to deploy the LoRA-finetuned LLMs on the hybrid compute-in-memory (CIM) architecture (i.e., pretrained weights onto RRAM and LoRA onto SRAM). To address performance degradation from RRAM’s inherent noise, we design a novel Hardware-aware Low-rank Adaption (HaLoRA) method, aiming to train a LoRA branch that is both robust and accurate by aligning the training objectives under both ideal and noisy conditions. Experiments finetuning LLaMA 3.2 1B and 3B demonstrate HaLoRA’s effectiveness across multiple reasoning tasks, achieving up to 22.7 improvement in average score while maintaining robustness at various noise levels.

Index Terms—low-rank adaptation, large language models, RRAM, SRAM

I. INTRODUCTION

Large language models (LLMs), such as GPT-4 [9], LLaMA [6], and Qwen [10], have demonstrated promising performance in various Natural Language Processing (NLP) tasks. However, this success, primarily driven by massive model parameters, brings forth two critical challenges in practical applications. First, adapting LLMs to downstream tasks via full model finetuning requires prohibitive computational resources. Second, model inference demands substantial energy consumption, limiting the wide deployment of these models.

Various parameter-efficient finetuning (PEFT) methods have been proposed to address the adaptation limitation [11]–[13]. Among them, low-rank adaptation (LoRA) [1] has gained increasing popularity due to its simplicity and efficacy by updating only an extra low-rank matrix while preserving the original pretrained weights. Meanwhile, to improve inference efficiency, Computing-in-Memory (CIM) architectures perform computations directly within memory arrays, achieving high energy efficiency through array-level parallel computing. Resistive random-access memory (RRAM) and static random-access memory (SRAM) are two typical memory devices used in CIM implementations. However, deploying LoRA-finetuned LLMs on CIM architectures remains largely unexplored, presenting both challenges and opportunities.

TABLE I: The comparison between the pretrained weight and LoRA branch when finetuning LLMs such as LLaMA 3.2 1B.

	Pretrained Weight	LoRA Branch
Parameters	1235.8M	1.9M
Task-agnostic	✓	✗
Trainable	✗	✓
CIM	RRAM	SRAM

In this paper, we propose a hybrid deployment strategy that leverages the complementary advantages of RRAM-based and SRAM-based CIM architectures. Pure RRAM-based CIM achieves high energy efficiency but suffers from inherent noise characteristics and complex write-verify operations [15], while pure SRAM-based CIM provides noise-free computation but is limited by its volatile nature and low storage density [16]. LoRA-finetuned LLMs exhibit a distinctive structural characteristic: as shown in Table I, the pretrained weights (e.g., 1235.8M parameters in LLaMA 3.2 1B) dominate the model size compared to the LoRA branch (1.9M parameters). Our hybrid strategy exploits this characteristic: 1) deploying the task-agnostic pretrained weights on RRAM maximizes energy efficiency while avoiding frequent write operations, and 2) implementing the task-specific LoRA branches on SRAM ensures accurate adaptation at a reasonable cost. Despite RRAM’s energy efficiency, the inherent non-ideality would introduce noise during the reading process, misleading the model to generate nonsense responses (shown in Fig. 1). These raise an intriguing question: *Can we leverage the accurate LoRA computations on SRAM to compensate for the noise-induced errors from pretrained weights deployed on RRAM, thereby achieving an optimal balance between energy efficiency and task adaptation?*

To this end, we propose Hardware-aware Low-Rank Adaptation (HaLoRA), a noise-robust adaptation method. Our key insight is to minimize the discrepancy of two LoRA optimization directions with and without noise in pretrained weights during training, and thus the optimized LoRA would be both **robust (via aware of noise)** and **accurate (via minimizing the gap)**. We first inject random noise into the pretrained weights and then optimize the LoRA branches

[†]Equal Contributions. ^{*}Corresponding authors.

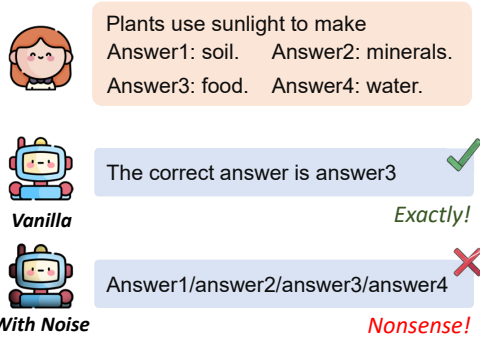


Fig. 1: One case during inference for noise-free and noisy LoRA-finetuned LLMs. The non-ideality of RRAM imposes noise on pretrained weights and thus hurts the performance.

towards the noise-free optimal to avoid overfitting to specific noise patterns. With a theoretically proven noise-agnostic upper bound of this optimization gap, HaLoRA achieves superior performance under noisy pretrained weights during inference.

We conduct comprehensive experiments by finetuning LLaMA 3.2 (1B and 3B variants) on commonsense reasoning tasks. To evaluate robustness, we inject noise into pretrained weights at three different levels during inference, with each condition tested across five random seeds. Experimental results demonstrate that HaLoRA consistently outperforms standard LoRA. Most notably, at a noise level of 0.02, HaLoRA achieves an average score of 63.1, surpassing LoRA by a significant margin of 22.7 points. These results validate our approach’s effectiveness in deploying LLMs on hybrid CIM architectures while maintaining robust performance. Our contributions can be summarized as follows:

- We propose the first framework to deploy LoRA-finetuned LLMs on the hybrid CIM architecture, i.e., task-agnostic pretrained weights onto RRAM and task-specific LoRA onto SRAM.
- We introduce HaLoRA which addresses RRAM non-ideality issues and guarantees accurate outputs by aligning noisy and noise-free training objectives with theoretical performance guarantees.
- We evaluate HaLoRA by finetuning LLaMA 3.2 (1B and 3B variants) on commonsense reasoning tasks, demonstrating the effectiveness and robustness of the proposed HaLoRA.

II. RELATED WORK

A. LoRA and its Variants

PEFT methods aim to update a small proportion of parameters to adapt LLMs for downstream tasks [1], [2], [11]–[13]. Among these methods, LoRA [1], which injects trainable low-rank branches to approximate the weight updates, has become increasingly popular as introducing no latency during inference. In the vanilla LoRA method, the authors introduce two linear projection layers and initialize them as Kaiming uniform and zero matrices [1]. The following variants can

be categorized into: 1) searching ranks [4]; 2) introducing training skills such as setting different learning rates [?]; and 3) designing new structures, such as [2]. However, all these variants focus on improving performance for the ideal scenarios without weight noise. In this paper, we propose HaLoRA, which is customized for hardware deployment.

B. Hybrid CIM Architecture

Hybrid CIM architectures combine different memory devices to achieve capabilities beyond what pure single-memory-device architectures can offer. Among them, RRAM-SRAM hybrid architectures have attracted significant attention by combining the high energy efficiency of RRAM with accurate computation of SRAM [29]–[32]. These hybrid designs typically partition computational tasks based on the characteristics of each memory device: deploying high-precision, frequently updated operations on SRAM while allocating computation-intensive yet structurally simple operations to RRAM [32]. This strategy has facilitated the efficient implementation of convolutional neural networks (CNNs) and lightweight neural architectures [17], [19], [29], enabling their deployment in edge computing applications such as robotic localization [18], target tracking [20], and recommendation systems [21]. However, existing hybrid architectures primarily focus on implementing small-scale models, with limited exploration of large language models. In this work, we explore efficient LLM deployment with hybrid CIM architecture.

C. Robustness Methods against Hardware Non-idealities

The robustness methods against the RRAM non-idealities have been a hot topic for the past decade. Specifically, these robust methods can be categorized into 1) noise-aware training, which typically incorporates noise during the training process or introduces robust loss functions [34]–[36], and 2) hardware compensation strategies, such as mapping critical weights to low-variation areas [38], [39]. However, these methods mainly focus on the robustness of convolutional neural networks (CNNs) and are hard to generalize to LLMs. Considering noise-aware training methods, the key is to continuously train the models to improve their robustness including knowledge distillation [36] and Bayesian neural network training [34], [35]. Due to the massive size of the LLM model, such as 3 billion parameters [6], the cost of continuous training is unaffordable. Meanwhile, the hardware compensation strategies are impractical for LLMs since pre-testing and correcting each layer through input regularization and column-shared factors introduce substantial additional hardware overhead. In this paper, we focus on improving the robustness of LoRA-finetuned LLMs at the finetuning stage.

III. METHODOLOGY

This section first introduces the preliminary about Transformer and LoRA, followed by the details of the deployment strategy and training process via the proposed HaLoRA.

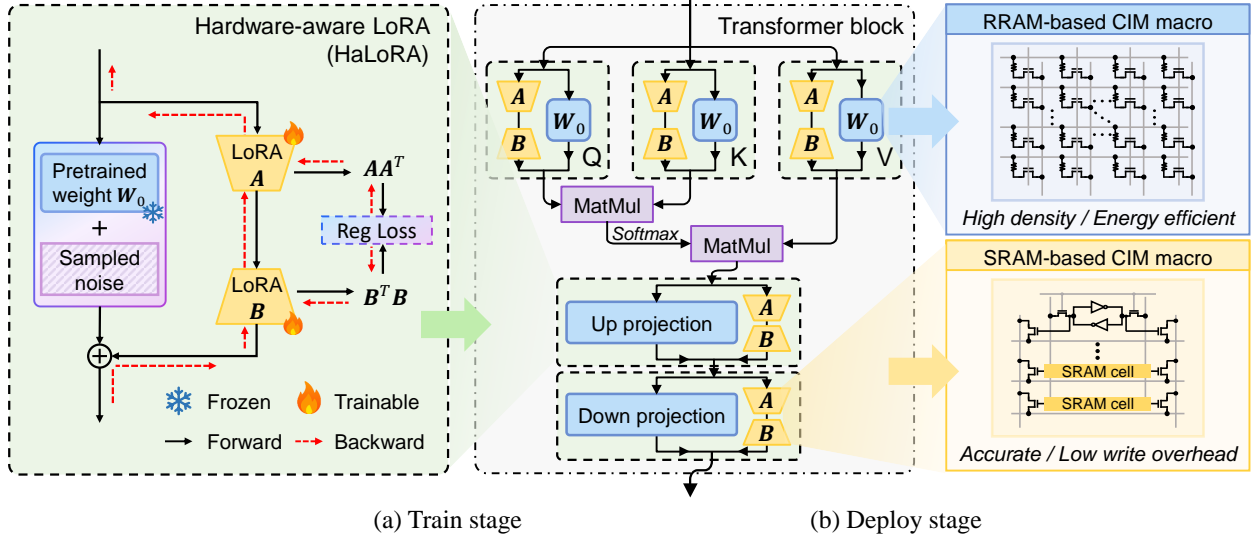


Fig. 2: The train and deploy stages for proposed HaLoRA. (a) During the training stage, HaLoRA incorporates an additional loss regularization term with sampled noise to enhance model robustness. (b) In the deploy stage, the finetuned LLM is mapped to a hybrid CIM architecture formed by RRAM and SRAM-based CIM macros, leveraging their respective advantages.

A. Preliminary

Transformer. Transformer [5] is the predominant architecture for LLMs, such as LLaMA [6]. Each transformer layer consists of a multi-head self-attention (MHA) sub-layer and a feed-forward (FFN) sub-layer. In the MHA sublayer, the input would be projected into K, Q, and V vectors, followed by the nonparametric operations. Then, the FFN sublayer contains an up-projection linear layer and a down-projection linear layer. We refer the readers to [7] for more details.

Vanilla LoRA. Based on the observation that the update in pretrained weights during model adaptation exhibits low intrinsic rank, the LoRA [1] method aims to model the weight update $\Delta \mathbf{W}$ of weight $\mathbf{W}_0 \in \mathbb{R}^{d_1 \times d_2}$ via two low-rank matrices following:

$$\mathbf{W} = \mathbf{W}_0 + \Delta \mathbf{W}, \quad \Delta \mathbf{W} = \mathbf{AB} \in \mathbb{R}^{d_1 \times d_2}, \quad (1)$$

where $\mathbf{A} \in \mathbb{R}^{d_1 \times r}$ and $\mathbf{B} \in \mathbb{R}^{r \times d_2}$. The parameters to update would be much less since we have $(d_1 + d_2)r \ll d_1 \times d_2$ when $r \ll \min(d_1, d_2)$. During finetuning, we would update the LoRA branch (i.e., \mathbf{A} and \mathbf{B}) while freezing the original pretrained weight \mathbf{W}_0 . Therefore, LoRA branches are task-specific while original pretrained weights are task-agnostic.

B. Impact simulation for Hybrid CIM

We propose a deployment strategy for finetuned LLMs in a hybrid CIM architecture that exploits the complementary strengths of RRAM and SRAM. As shown in Fig. 2b, the architecture implements the LLM backbone in RRAM, leveraging its storage density and energy efficiency. The noise-sensitive and task-specific LoRA branch is deployed on SRAM for accurate write operations and efficient task adaptation. For attention blocks, while previous works [22], [23] demonstrate fully RRAM-based deployment, the dynamic matrix-matrix

multiplication (MatMul) requires extensive write-verify operations during inference. To achieve efficient dynamic matrix operations, the MatMul modules are allocated to SRAM for lower memory writing overhead.

In the context of neural network inference tasks, hardware non-ideality primarily manifests as random noise arising from device variability [25]. Empirical evidence from previous research has demonstrated that such noise can be safely modeled as zero-mean Gaussian noise [24]. While computations of LoRA branches on SRAM-CIM maintain high precision due to digital computing, noise effects on the LLM backbone executed on RRAM-CIM require special consideration.

To address this challenge, we implement a block-wise linear mapping strategy that aligns with practical deployment workflows [25] and introduces noise into the weights of individual sub-blocks to accurately simulate the impact of analog computing noise. For the target RRAM tiles in the shape of $m \times n$, the magnitude of the simulated Gaussian noise is determined by the device-specific standard deviation σ . Thus, the non-ideality simulation of RRAM-CIM macros acting on weight matrix $\mathbf{W}_0 \in \mathbb{R}^{d_1 \times d_2}$ can be formulated as:

$$\{\mathbf{W}_{0,[i,j]}\}_{i=1,j=1}^{k,t} = \text{split}(\mathbf{W}_0), \quad k = \lceil \frac{d_1}{m} \rceil, \quad t = \lceil \frac{d_2}{n} \rceil, \quad (2)$$

$$\mathbf{W}_0^* = \text{cat}(\{\mathbf{W}_{0,[i,j]} + \lambda(\max(\text{abs}(\mathbf{W}_{0,[i,j]})))\}_{i=1,j=1}^{k,t}), \quad \lambda \sim \mathcal{N}(0, \sigma) \quad (3)$$

where $\text{split}(\cdot)$ and $\text{cat}(\cdot)$ denote the matrix splitting and concatenation operations respectively, $\mathbf{W}_{0,[i,j]}$ represents the partitioned weight block, and \mathbf{W}_0^* corresponds to the noise-injected weight matrix.

These approaches ensure simulation results that reflect the practical constraints and capabilities of the hybrid architecture.

Algorithm 1 HaLoRA

Input: Train data \mathcal{D}_{train} , Finetuned LLM M
Params: N : steps to apply alignment, μ : loss weight for regularization loss
Output: Updated LoRA branch.

- 1: Insert LoRA for selected linear layer in M
- 2: Initialize LoRA branch where \mathbf{A} as Kaiming Uniform distribution and \mathbf{B} as Zero matrix.
- 3: Sample Noise to pretrained weight \mathbf{W}_0 following Equation 3
- 4: **for** $i = 0$ to max training steps **do**
- 5: Forward a batch from \mathcal{D}_{train} through M , derive the gradients g_{ori} for LoRA to update following Equation 4
- 6: **if** $i \% N == 0$ **then**
- 7: Sample Noise to pretrained weight \mathbf{W}_0 following Equation 3
- 8: Calculate regularization loss \mathcal{L}_{reg} following Equation 10
- 9: backward loss to get the regularization gradient g_{reg}
- 10: $g_{ori} \leftarrow g_{ori} + \mu g_{reg}$
- 11: **end if**
- 12: Update the LoRA branch with corresponding g_{ori} while keeping \mathbf{W}_0 frozen
- 13: **end for**
- 14: **return** Optimized the LoRA branch

C. Hardware-aware Low-Rank Adaptation (HaLoRA)

In the hybrid CIM architecture, the inherent noise from RRAM would lead to performance degradation. Specifically, as shown in Table II, the noise at the level of $\sigma = 0.02$ would decrease the average scores by 21.7 and 15.8 for the LLaMA 3.2 1B and 3B model, respectively.

To address this issue, we propose a novel HaLoRA method. The key insight is to align the training objectives under both ideal and noisy conditions during the training process, and thus train a better LoRA branch that is both robust to the noise (via aware of noise) and accurate (via minimizing the gap) during inference.

Considering the gradients for matrices \mathbf{A} and \mathbf{B} in LoRA, we have:

$$\frac{\partial \mathcal{L}}{\partial \mathbf{A}} = \frac{\partial \mathcal{L}}{\partial \mathbf{W}} \mathbf{B}^T, \quad \frac{\partial \mathcal{L}}{\partial \mathbf{B}} = \mathbf{A}^T \frac{\partial \mathcal{L}}{\partial \mathbf{W}}, \quad (4)$$

where \mathbf{W} is the merged weight defined in Equation 1. For the ideal condition without noise, the updated LoRA branch can be formulated as:

$$\begin{aligned} (\mathbf{A} - \eta \frac{\partial \mathcal{L}}{\partial \mathbf{A}})(\mathbf{B} - \eta \frac{\partial \mathcal{L}}{\partial \mathbf{B}}) &= (\mathbf{A} - \eta \frac{\partial \mathcal{L}}{\partial \mathbf{W}} \mathbf{B}^T)(\mathbf{B} - \eta \mathbf{A}^T \frac{\partial \mathcal{L}}{\partial \mathbf{W}}) \\ &\approx \mathbf{AB} - \eta \mathbf{AA}^T \frac{\partial \mathcal{L}}{\partial \mathbf{W}} - \eta \frac{\partial \mathcal{L}}{\partial \mathbf{W}} \mathbf{B}^T \mathbf{B}, \end{aligned} \quad (5)$$

where η is the learning rate such as 1e-3 and thus we discard the item $\eta^2 \frac{\partial \mathcal{L}}{\partial \mathbf{W}} \mathbf{B}^T \mathbf{A}^T \frac{\partial \mathcal{L}}{\partial \mathbf{W}}$. Considering the noise existed in \mathbf{W}_0 , we have:

$$\mathbf{W}^* = \mathbf{W}_0^* + \Delta \mathbf{W}. \quad (6)$$

Similarly, we can thus get the updated LoRA branch under the same initialization:

$$\begin{aligned} (\mathbf{A} - \eta \frac{\partial \mathcal{L}}{\partial \mathbf{A}})(\mathbf{B} - \eta \frac{\partial \mathcal{L}}{\partial \mathbf{B}}) &= (\mathbf{A} - \eta \frac{\partial \mathcal{L}}{\partial \mathbf{W}^*} \mathbf{B}^T)(\mathbf{B} - \eta \mathbf{A}^T \frac{\partial \mathcal{L}}{\partial \mathbf{W}^*}) \\ &\approx \mathbf{AB} - \eta \mathbf{AA}^T \frac{\partial \mathcal{L}}{\partial \mathbf{W}^*} - \eta \frac{\partial \mathcal{L}}{\partial \mathbf{W}^*} \mathbf{B}^T \mathbf{B}. \end{aligned} \quad (7)$$

To align the optimization process under ideal and noisy conditions, we aim to minimize the gap between Equation 5 and Equation 7, which can be formulated as:

$$\min \eta \|\mathbf{AA}^T(\frac{\partial \mathcal{L}}{\partial \mathbf{W}^*} - \frac{\partial \mathcal{L}}{\partial \mathbf{W}}) + (\frac{\partial \mathcal{L}}{\partial \mathbf{W}^*} - \frac{\partial \mathcal{L}}{\partial \mathbf{W}})\mathbf{B}^T \mathbf{B}\|. \quad (8)$$

The learning rate η is fixed and can be discarded. Given the property that $\|\mathbf{XY}\| \leq \|\mathbf{X}\| \|\mathbf{Y}\|$ and $\|\mathbf{X} + \mathbf{Y}\| \leq \|\mathbf{X}\| + \|\mathbf{Y}\|$, we can instead optimize the upper bound:

$$\begin{aligned} \min \|\mathbf{AA}^T\| \|\frac{\partial \mathcal{L}}{\partial \mathbf{W}^*} - \frac{\partial \mathcal{L}}{\partial \mathbf{W}}\| + \|\frac{\partial \mathcal{L}}{\partial \mathbf{W}^*} - \frac{\partial \mathcal{L}}{\partial \mathbf{W}}\| \|\mathbf{B}^T \mathbf{B}\| \\ \rightarrow \min \|\frac{\partial \mathcal{L}}{\partial \mathbf{W}^*} - \frac{\partial \mathcal{L}}{\partial \mathbf{W}}\| (\|\mathbf{AA}^T\| + \|\mathbf{B}^T \mathbf{B}\|). \end{aligned} \quad (9)$$

Since noise is stochastic and within a scope, then the optimization target can be defined as:

$$\min \|\mathbf{AA}^T\| + \|\mathbf{B}^T \mathbf{B}\|. \quad (10)$$

Finally, the goal to align the training process is simplified into Equation 10, which is *agnostic* from the noise. In HaLoRA, we select the Euclidean norm. As shown in Fig. 2(a), The training loss to update the LoRA branch is:

$$\mathcal{L}_{total} = \mathcal{L} + \mu \mathcal{L}_{reg}, \quad (11)$$

where μ is the hyperparameter for loss weight and $\mathcal{L}_{reg} = \|\mathbf{AA}^T\|_2 + \|\mathbf{B}^T \mathbf{B}\|_2$. Algorithm 1 indicates the details of the proposed HaLoRA.

IV. EXPERIMENTS

In this section, we conducted a comprehensive comparison between vanilla LoRA and HaLoRA using popular open-source LLaMA models across various benchmarks under different noise configurations.

A. Experimental Setup

Non-ideal effect simulation. In the hybrid CIM architecture, we consider the inference results based on digital SRAM macros to be relatively accurate. For the analog RRAM macros, based on noise levels reported in published RRAM chip studies [26], [27], the standard deviation of the injected Gaussian noise can be determined within the range of 0.01 to 0.02. To comprehensively evaluate practical noise mitigation strategies, including redundant mapping and bit-splitting techniques, we extended our validation to encompass lower noise levels ($\sigma = 0.005, 0.01$, and 0.02). Additionally, following the

TABLE II: The comparison between vanilla LoRA and HaLoRA on six popular benchmarks when finetuning LLaMA 3.2 1B and 3B on commonsense reasoning tasks. Compared to vanilla LoRA, HaLoRA performs better under the noise-free setting and showcases better robustness at all noise levels.

Model	Method	Noise	ARC-e	OBQA	SIQA	ARC-c	WinoG.	PIQA	Avg.
LLaMA 3.2 1B	LoRA	-	69.5	64.4	61.0	46.7	57.8	74.2	62.3
		5e-3	67.1 \pm 3.2	59.4 \pm 4.1	59.6 \pm 0.5	48.5 \pm 3.4	58.8 \pm 1.9	72.0 \pm 1.9	60.9
		1e-2	62.2 \pm 7.6	53.2 \pm 8.7	58.0 \pm 1.9	44.7 \pm 7.4	57.5 \pm 3.5	66.5 \pm 4.7	57.0
		2e-2	40.9 \pm 8.3	38.1 \pm 6.1	46.8 \pm 6.4	31.0 \pm 5.5	45.1 \pm 12.9	40.7 \pm 17.3	40.4
	HaLoRA	-	73.3	68.0	69.0	55.5	65.4	74.6	67.6
		5e-3	73.1 \pm 0.2	66.8 \pm 0.4	69.4 \pm 0.2	54.8 \pm 0.4	64.6 \pm 0.6	74.3 \pm 0.3	67.2
		1e-2	71.8 \pm 1.0	65.2 \pm 0.4	68.9 \pm 0.4	54.2 \pm 1.3	64.1 \pm 0.5	73.5 \pm 0.6	66.3
		2e-2	68.6 \pm 1.8	60.2 \pm 1.1	66.0 \pm 0.7	50.8 \pm 1.9	61.9 \pm 1.0	71.1 \pm 1.7	63.1
LLaMA 3.2 3B	LoRA	-	88.0	82.2	76.8	76.4	77.2	83.8	80.7
		5e-3	87.5 \pm 0.2	81.6 \pm 0.6	76.7 \pm 0.3	75.7 \pm 0.4	76.2 \pm 1.4	80.5 \pm 5.9	79.7
		1e-2	86.1 \pm 0.4	80.6 \pm 1.1	76.3 \pm 0.3	73.9 \pm 0.6	71.5 \pm 4.5	79.0 \pm 4.7	77.9
		2e-2	72.3 \pm 9.2	65.2 \pm 6.4	69.0 \pm 2.9	60.1 \pm 6.4	57.5 \pm 8.4	65.5 \pm 5.5	64.9
	HaLoRA	-	87.3	81.4	77.7	76.7	80.6	84.2	81.3
		5e-3	87.0 \pm 0.1	82.3 \pm 0.3	77.6 \pm 0.3	76.4 \pm 0.4	80.1 \pm 0.1	83.9 \pm 0.2	81.2
		1e-2	86.6 \pm 0.1	81.6 \pm 0.9	77.2 \pm 0.3	76.0 \pm 0.6	79.3 \pm 0.5	83.4 \pm 0.3	80.7
		2e-2	84.6 \pm 0.3	78.8 \pm 0.6	75.8 \pm 0.9	72.8 \pm 1.5	77.2 \pm 0.9	81.0 \pm 1.1	78.4

block-wise linear mapping characteristics of weights on physical RRAM crossbars [25], we partitioned the corresponding weights into 64×64 blocks to align with conventional memory tile dimensions. These blocks were then subjected to noise injection procedures (detailed in Section III-B).

HaLoRA finetuning. We conduct experiments on two variants of the LLaMA 3.2 family: LLaMA-1B and LLaMA-3B with 1.3 billion and 3.2 billion parameters, respectively. Following [14], we employ the 170k samples for training. As shown in Fig. 2, we insert the LoRA branches into five modules: query/key/value/up/down projection layers. The rank in LoRA is 4. For the random noise, we sample noise every 400 steps ($N = 400$) and set the noise level at 0.01. We train on a single NVIDIA A100 GPU with a batch size of 16 for 3 epochs while the learning rate is 1e-4. It takes around 2 hours to finetune the 1B version LLaMA 3.2.

Evaluation. We evaluate 6 popular benchmarks, including 1) ARC-e (Easy set of AI2 Reasoning Challenge), 2) OBQA (OpenBook Question Answering), 3) SIQA (Social Interaction QA), 4) ARC-c (Challenge set of AI2 Reasoning Challenge), 5) WinoG. (Winograd Schema Challenge), and 6) PIQA (Physical Interaction QA). We refer the readers to [2] for more details about these benchmarks. During inference, we sample the noise 5 times under the random seed $\{1,2,3,4,5\}$ for each noise level from $\{0.005, 0.01, 0.02\}$. Meanwhile, we also report the performance without noise. For all the benchmarks, both the average and standard deviation of accuracy are reported.

B. Main Results

Table II presents the results on 6 benchmarks when finetuning LLaMA 3.2 1B and 3B. For each benchmark, we

report the noise-free evaluation results and the average with standard deviation when adding noise. Besides, we also report the overall average of these average scores on 6 benchmarks. Some key findings can be summarized as:

- **HaLoRA demonstrates better performance at noise-free setting.** As LLMs inherently tend to overfit during dataset training [8], HaLoRA’s noise injection effectively enhances the diversity of model representations during the finetuning process, leading to improved performance on test sets. Specifically, under noise-free deployment conditions, HaLoRA achieves average performance improvements of 5.3 and 0.6 points compared to vanilla LoRA on LLaMA 1B and 3B models, respectively.
- **HaLoRA demonstrates superior accuracy at all noise levels.** Compared to vanilla LoRA, HaLoRA demonstrates enhanced performance across all six datasets. Notably, at a deployment noise level of 0.02, HaLoRA achieves substantial performance improvements over vanilla LoRA: 22.7 points (63.1 vs. 40.4) for LLaMA 3.2 1B and 13.5 points (78.4 vs. 64.9) for LLaMA 3.2 3B. Furthermore, HaLoRA shows significantly reduced performance degradation as noise levels increase. When noise levels escalate to 0.02, HaLoRA’s average performance degradation is only 21% (4.5 vs. 21.9 points) and 18% (2.9 vs. 15.8 points) of vanilla LoRA’s degradation for LLaMA 3.2 1B and 3B, respectively.
- **HaLoRA demonstrates superior stability under noisy conditions.** At identical noise levels, HaLoRA exhibits significantly lower performance variance across different noise directions. For LLaMA 1B, across five experimental runs, HaLoRA’s performance variance on WinoG. and PIQA datasets are merely 7% (1.0 vs. 12.9) and 10%

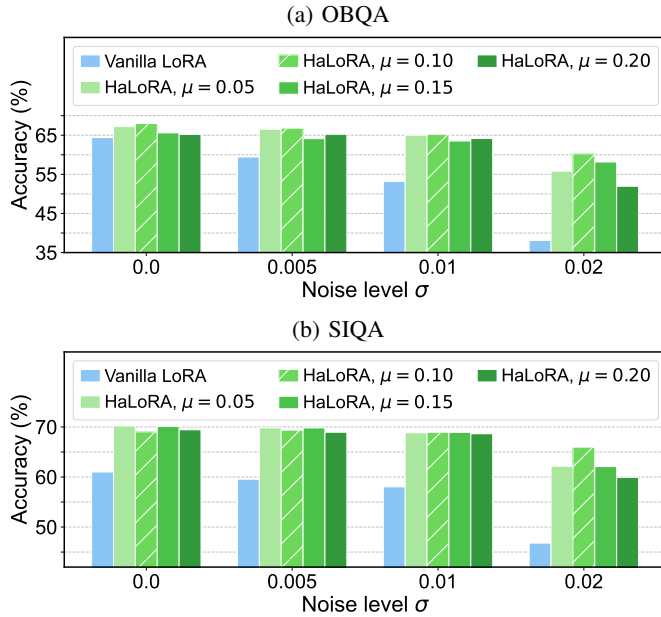


Fig. 3: The performance of HaLoRA with different values of μ and vanilla LoRA on the OBQA and SIQA datasets.

(1.7 vs. 17.3) of vanilla LoRA’s variance, respectively. Similarly, for LLaMA 3B, HaLoRA achieves remarkably lower variance on ARC-e and WinoG. datasets, showing only 3% (0.3 vs. 9.2) and 11% (0.9 vs. 8.4) of vanilla LoRA’s variance.

- **Larger model shows better robustness against noise.** Comparing the performance of LLaMA 3B and LLaMA 1B across multiple datasets under identical noise levels, both vanilla LoRA and HaLoRA (particularly the latter) exhibit reduced accuracy degradation in larger models (accuracy drops of 15.8 vs. 21.9 for vanilla LoRA, and 2.9 vs. 4.5 for HaLoRA). Additionally, larger models show more stable performance, as evidenced by lower standard deviations (maximum values of 5.5 vs. 17.3 for vanilla LoRA, and 1.5 vs. 1.9 for HaLoRA). These results suggest that the model scale positively correlates with noise resilience.

In summary, HaLoRA provides a robust solution for deploying fintuned LLMs on noisy hybrid architectures. Our findings also reveal that larger models (especially with HaLoRA) tend to demonstrate better tolerance to hardware-induced noise compared to the smaller models.

C. Further Analysis

Sensitivity of μ . We conducted a sensitivity analysis of hyperparameter μ on LLaMA 1B to further evaluate HaLoRA’s stability. Figures 3(a) and (b) illustrate the average performance scores across different noise levels and μ values on the OBQA and SIQA datasets with random seeds of 1 to 5, respectively.

TABLE III: Cases from LoRA-finetuned and HaLoRA-finetuned LLaMA 3.2 1B from the ARC-e datasets. **Blue** for right answers and **red** for wrong.

Input #1	The Apollo 11 mission was able to retrieve samples of the Moon’s surface because it was the first mission to have astronauts: Answer1: land on the Moon Answer2: orbit a planet Answer3: return to Earth Answer4: walk in space
Ground Truth	Answer1
	<i>Noise-free</i>
LoRA	The correct answer is Answer1
HaLoRA (Ours)	The correct answer is Answer1
	<i>Noise ($\sigma=2e-2$)</i>
LoRA	1/2/3/4
HaLoRA (Ours)	The correct answer is Answer1
Input #2	Please choose the correct answer to the question: When trees develop leaves in the spring, 10 changes occur on the forest floor. Why does the development of leaves cause changes on the forest floor? Answer1: Rainfall increases. Answer2: Sunlight is reduced. Answer3: Wind speed increases. Answer4: Animal migration is stopped.
Ground Truth	Answer2
	<i>Noise-free</i>
LoRA	The correct answer is Answer1
HaLoRA (Ours)	The correct answer is Answer2
	<i>Noise ($\sigma=2e-2$)</i>
LoRA	Answer1/Answer2/Answer3/Answer4 is the correct answer. Answer1
HaLoRA (Ours)	The correct answer is Answer2

Overall, HaLoRA demonstrates relatively stable performance across different values of μ . Although the performance variations slightly increase with higher noise levels, the average results from five experiments show that μ within the range of [0.05, 0.15] lead to maximum performance changes of 4.4 and 3.9 points on OBQA and SIQA, respectively. Notably, HaLoRA consistently outperforms Vanilla LoRA across all values of μ .

As μ increases from smaller to larger values, we observe distinct behavioral patterns. Smaller μ enhances the LoRA branch’s noise tolerance at the finetuning noise level but leads to performance degradation when the noise level exceeds the finetuning setting ($\sigma = 0.02 > 0.005$). Conversely, excessively large μ leads to overfitting to precise outputs, compromising the network’s inherent noise-tolerant capabilities.

Case study. We showcase the outputs of LoRA and HaLoRA with and without noise, respectively. Table III indicates the cases from the ARC-e dataset. We can find that noise would lead to the nonsense output from the LoRA-finetuned LLaMA 3.2 1B, while the HaLoRA-finetuned one shows strong robustness capability. Moreover, considering the noise-free setting of case #2, HaLoRA-finetuned LLaMA 3.2 1B can generate the right answer while LoRA-finetuned one would fail. This phenomenon is consistent with Table II that HaLoRA demonstrates better performance under a noise-free setting.

Specifically, HaLoRA gets an average score of 67.6, which is higher than the 62.3 of LoRA.

V. CONCLUSION

In this work, we present a hybrid CIM architecture for deploying LoRA-finetuned LLMs based on both RRAM and SRAM devices. Through theoretical analysis of device noise impact on LLM inference, we identify the performance degradation caused by RRAM non-ideality as a key challenge. To address this issue, we propose HaLoRA, which aligns the training objectives under both ideal and noisy conditions and optimizes the upper bound of the alignment loss. Experimental results demonstrate that HaLoRA consistently enhances LLM performance when deployed on noisy hybrid architectures. For future work, we plan to extend HaLoRA to quantized LLMs and explore its effectiveness in more challenging tasks such as mathematical reasoning.

REFERENCES

- [1] E. J. Hu, P. Wallis, Z. Allen-Zhu, Y. Li, S. Wang, L. Wang, W. Chen, *et al.*, “Lora: Low-rank adaptation of large language models,” in *International Conference on Learning Representations*, 2022.
- [2] T. Wu, J. Wang, Z. Zhao, and N. Wong, “Mixture-of-subspaces in low-rank adaptation,” *arXiv preprint arXiv:2406.11909*, 2024.
- [3] S. Hayou, N. Ghosh, and B. Yu, “LORA+: Efficient low rank adaptation of large models,” in *Proceedings of the 41st International Conference on Machine Learning* (R. Salakhutdinov, Z. Kolter, K. Heller, A. Weller, N. Oliver, J. Scarlett, and F. Berkenkamp, eds.), vol. 235 of *Proceedings of Machine Learning Research*, pp. 17783–17806, PMLR, 21–27 Jul 2024.
- [4] Q. Zhang, M. Chen, A. Bukharin, N. Karampatziakis, P. He, Y. Cheng, W. Chen, and T. Zhao, “Adalora: Adaptive budget allocation for parameter-efficient fine-tuning,” 2023.
- [5] A. Vaswani, N. Shazeer, N. Parmar, J. Uszkoreit, L. Jones, A. N. Gomez, L. Kaiser, and I. Polosukhin, “Attention is all you need,” *Advances in Neural Information Processing Systems*, 2017.
- [6] A. Dubey, A. Jauhri, A. Pandey, A. Kadian, A. Al-Dahle, A. Letman, A. Mathur, A. Schelten, A. Yang, A. Fan, *et al.*, “The llama 3 herd of models,” *arXiv preprint arXiv:2407.21783*, 2024.
- [7] T. Wu, C. Hou, S. Lao, J. Li, N. Wong, Z. Zhao, and Y. Yang, “Weight-inherited distillation for task-agnostic bert compression,” *arXiv preprint arXiv:2305.09098*, 2023.
- [8] C. Wu, F. Wu, T. Qi, Y. Huang, and X. Xie, “Noisytune: A little noise can help you finetune pretrained language models better,” *arXiv preprint arXiv:2202.12024*, 2022.
- [9] J. Achiam, S. Adler, S. Agarwal, L. Ahmad, I. Akkaya, F. L. Aleman, D. Almeida, J. Altenschmidt, S. Altman, S. Anadkat, *et al.*, “Gpt-4 technical report,” *arXiv preprint arXiv:2303.08774*, 2023.
- [10] J. Bai, S. Bai, Y. Chu, Z. Cui, K. Dang, X. Deng, Y. Fan, W. Ge, Y. Han, F. Huang, *et al.*, “Qwen technical report,” *arXiv preprint arXiv:2309.16609*, 2023.
- [11] N. Houlsby, A. Giurgiu, S. Jastrzebski, B. Morrone, Q. De Laroussilhe, A. Gesmundo, M. Attariyan, and S. Gelly, “Parameter-efficient transfer learning for nlp,” in *International conference on machine learning*, pp. 2790–2799, PMLR, 2019.
- [12] X. L. Li and P. Liang, “Prefix-tuning: Optimizing continuous prompts for generation,” *arXiv preprint arXiv:2101.00190*, 2021.
- [13] E. B. Zaken, S. Ravfogel, and Y. Goldberg, “Bitfit: Simple parameter-efficient fine-tuning for transformer-based masked language-models,” *arXiv preprint arXiv:2106.10199*, 2021.
- [14] Z. Hu, L. Wang, Y. Lan, W. Xu, E.-P. Lim, L. Bing, X. Xu, S. Poria, and R. K.-W. Lee, “Llm-adapters: An adapter family for parameter-efficient fine-tuning of large language models,” *arXiv preprint arXiv:2304.01933*, 2023.
- [15] D. Ielmini and H.-S. P. Wong, “In-memory computing with resistive switching devices,” *Nature electronics*, vol. 1, no. 6, pp. 333–343, 2018.
- [16] A. Sebastian, M. Le Gallo, R. Khaddam-Aljameh, and E. Eleftheriou, “Memory devices and applications for in-memory computing,” *Nature nanotechnology*, vol. 15, no. 7, pp. 529–544, 2020.
- [17] M. Chang, S. D. Spetnich, B. Crafton, W.-S. Khwa, Y.-D. Chih, M.-F. Chang, and A. Raychowdhury, “A 40nm 60.64tops/w ecc-capable compute-in-memory/digital 2.25mb/768kb rram/sram system with embedded cortex m3 microprocessor for edge recommendation systems,” in *2022 IEEE International Solid-State Circuits Conference (ISSCC)*, vol. 65, pp. 1–3, 2022.
- [18] S. D. Spetnich, A. S. Lele, B. Crafton, M. Chang, S. Ryu, J.-H. Yoon, Z. Hao, A. Ansari, W.-S. Khwa, Y.-D. Chih, M.-F. Chang, and A. Raychowdhury, “30.1 a 40nm vliw edge accelerator with 5mb of 0.256pj/b rram and a localization solver for bristle robot surveillance,” in *2024 IEEE International Solid-State Circuits Conference (ISSCC)*, vol. 67, pp. 482–484, 2024.
- [19] K. Prabhu, A. Gural, Z. F. Khan, R. M. Radway, M. Giordano, K. Koul, R. Doshi, J. W. Kustin, T. Liu, G. B. Lopes, V. Turbiner, W.-S. Khwa, Y.-D. Chih, M.-F. Chang, G. Lallement, B. Murmann, S. Mitra, and P. Raina, “Chimera: A 0.92-tops, 2.2-tops/w edge ai accelerator with 2-mbyte on-chip foundry resistive ram for efficient training and inference,” *IEEE Journal of Solid-State Circuits*, vol. 57, no. 4, pp. 1013–1026, 2022.
- [20] M. Chang, A. S. Lele, S. D. Spetnich, B. Crafton, S. Konno, Z. Wan, A. Bhat, W.-S. Khwa, Y.-D. Chih, M.-F. Chang, and A. Raychowdhury, “A 73.53tops/w 14.74tops heterogeneous rram in-memory and sram near-memory soc for hybrid frame and event-based target tracking,” in *2023 IEEE International Solid-State Circuits Conference (ISSCC)*, pp. 426–428, 2023.
- [21] M. Chang, S. D. Spetnich, B. Crafton, W.-S. Khwa, Y.-D. Chih, M.-F. Chang, and A. Raychowdhury, “A 40nm 60.64tops/w ecc-capable compute-in-memory/digital 2.25mb/768kb rram/sram system with embedded cortex m3 microprocessor for edge recommendation systems,” in *2022 IEEE International Solid-State Circuits Conference (ISSCC)*, vol. 65, pp. 1–3, 2022.
- [22] X. Yang, B. Yan, H. Li, and Y. Chen, “Retransformer: Reram-based processing-in-memory architecture for transformer acceleration,” in *2020 IEEE/ACM International Conference On Computer Aided Design (ICCAD)*, pp. 1–9, 2020.
- [23] C. Yang, X. Wang, and Z. Zeng, “Full-circuit implementation of transformer network based on memristor,” *IEEE Transactions on Circuits and Systems I: Regular Papers*, vol. 69, no. 4, pp. 1395–1407, 2022.
- [24] Z. Yan, X. S. Hu, and Y. Shi, “Swim: Selective write-verify for computing-in-memory neural accelerators,” in *Proceedings of the 59th ACM/IEEE Design Automation Conference*, pp. 277–282, 2022.
- [25] X. Peng, S. Huang, Y. Luo, X. Sun, and S. Yu, “Dnn+neurosim: An end-to-end benchmarking framework for compute-in-memory accelerators with versatile device technologies,” in *2019 IEEE International Electron Devices Meeting (IEDM)*, pp. 32.5.1–32.5.4, 2019.
- [26] P. Yao, H. Wu, B. Gao, J. Tang, Q. Zhang, W. Zhang, J. J. Yang, and H. Qian, “Fully hardware-implemented memristor convolutional neural network,” *Nature*, vol. 577, no. 7792, pp. 641–646, 2020.
- [27] Y. Liu, B. Gao, J. Tang, H. Wu, and H. Qian, “Architecture-circuit-technology co-optimization for resistive random access memory-based computation-in-memory chips,” *Science China Information Sciences*, vol. 66, no. 10, p. 200408, 2023.
- [28] C. Yu, T. Yoo, K. T. C. Chai, T. T.-H. Kim, and B. Kim, “A 65-nm 8t sram compute-in-memory macro with column adcs for processing neural networks,” *IEEE Journal of Solid-State Circuits*, vol. 57, no. 11, pp. 3466–3476, 2022.
- [29] K. Prabhu, R. M. Radway, Y. Jeffrey, K. Bartolone, M. Giordano, F. Peddinghaus, Y. Urman, W.-S. Khwa, Y.-D. Chih, M.-F. Chang, *et al.*, “Minotaur: An edge transformer inference and training accelerator with 12 mbytes on-chip resistive ram and fine-grained spatiotemporal power gating,” in *2024 IEEE Symposium on VLSI Technology and Circuits (VLSI Technology and Circuits)*, pp. 1–2, IEEE, 2024.
- [30] S. Liu, C. Mu, H. Jiang, Y. Wang, J. Zhang, F. Lin, K. Zhou, Q. Liu, and C. Chen, “Hardsea: Hybrid analog-reram clustering and digital-sram in-memory computing accelerator for dynamic sparse self-attention in transformer,” *IEEE Transactions on Very Large Scale Integration (VLSI) Systems*, 2023.
- [31] G. Krishnan, Z. Wang, I. Yeo, L. Yang, J. Meng, M. Liehr, R. V. Joshi, N. C. Cady, D. Fan, J.-S. Seo, *et al.*, “Hybrid rram/sram in-memory computing for robust dnn acceleration,” *IEEE Transactions on Computer-Aided Design of Integrated Circuits and Systems*, vol. 41, no. 11, pp. 4241–4252, 2022.
- [32] T.-H. Wen, J.-M. Hung, W.-H. Huang, C.-J. Jhang, Y.-C. Lo, H.-H. Hsu, Z.-E. Ke, Y.-C. Chen, Y.-H. Chin, C.-I. Su, *et al.*, “Fusion of memristor

and digital compute-in-memory processing for energy-efficient edge computing," *Science*, vol. 384, no. 6693, pp. 325–332, 2024.

- [33] T. Liu, W. Wen, L. Jiang, Y. Wang, C. Yang, and G. Quan, "A Fault-Tolerant Neural Network Architecture," in *2019 56th ACM/IEEE Design Automation Conference (DAC)*, pp. 1–6, 2019.
- [34] D. Gao, Q. Huang, G. L. Zhang, X. Yin, B. Li, U. Schlichtmann, and C. Zhuo, "Bayesian Inference Based Robust Computing on Memristor Crossbar," in *2021 58th ACM/IEEE Design Automation Conference (DAC)*, pp. 121–126, 2021.
- [35] N. Ye, J. Mei, Z. Fang, Y. Zhang, Z. Zhang, H. Wu, and X. Liang, "BayesFT: Bayesian Optimization for Fault Tolerant Neural Network Architecture," in *2021 58th ACM/IEEE Design Automation Conference (DAC)*, pp. 487–492, 2021.
- [36] G. Charan, J. Hazra, K. Beckmann, X. Du, G. Krishnan, R. V. Joshi, N. C. Cady, and Y. Cao, "Accurate Inference with Inaccurate RRAM Devices: Statistical Data, Model Transfer, and On-line Adaptation," in *2020 57th ACM/IEEE Design Automation Conference (DAC)*, pp. 1–6, 2020.
- [37] H. Shin, M. Kang, and L.-S. Kim, "Fault-free: A Fault-resilient Deep Neural Network Accelerator based on Realistic ReRAM Devices," in *2021 58th ACM/IEEE Design Automation Conference (DAC)*, pp. 1039–1044, 2021.
- [38] A. Malhotra, C. Wang, and S. K. Gupta, "TFix: Exploiting the Natural Redundancy of Ternary Neural Networks for Fault Tolerant In-Memory Vector Matrix Multiplication," in *2023 60th ACM/IEEE Design Automation Conference (DAC)*, pp. 1–6, 2023.
- [39] M. Lee, W. Tang, Y. Chen, J. Wu, H. Zhong, Y. Xu, Y. Liu, H. Yang, V. Narayanan, and X. Li, "Victor: A Variation-resilient Approach Using Cell-Clustered Charge-domain computing for High-density High-throughput MLC CiM," in *2023 60th ACM/IEEE Design Automation Conference (DAC)*, pp. 1–6, 2023.